UCRL-JC-106121
PREPRINT

Acceleration of Compact Toruses and Fusion Applications

C. W. Hartman, J. L. Eddleman, J. H. Hammer,
B. G. Logan, H. S. McLean, and A. W. Mólvik

This paper was prepared for presentation at the
Workshop on Physics of Alternative Magnetic
Confinement Schemes

Varenna, Italy

October 15-24, 1990

October 11, 1990

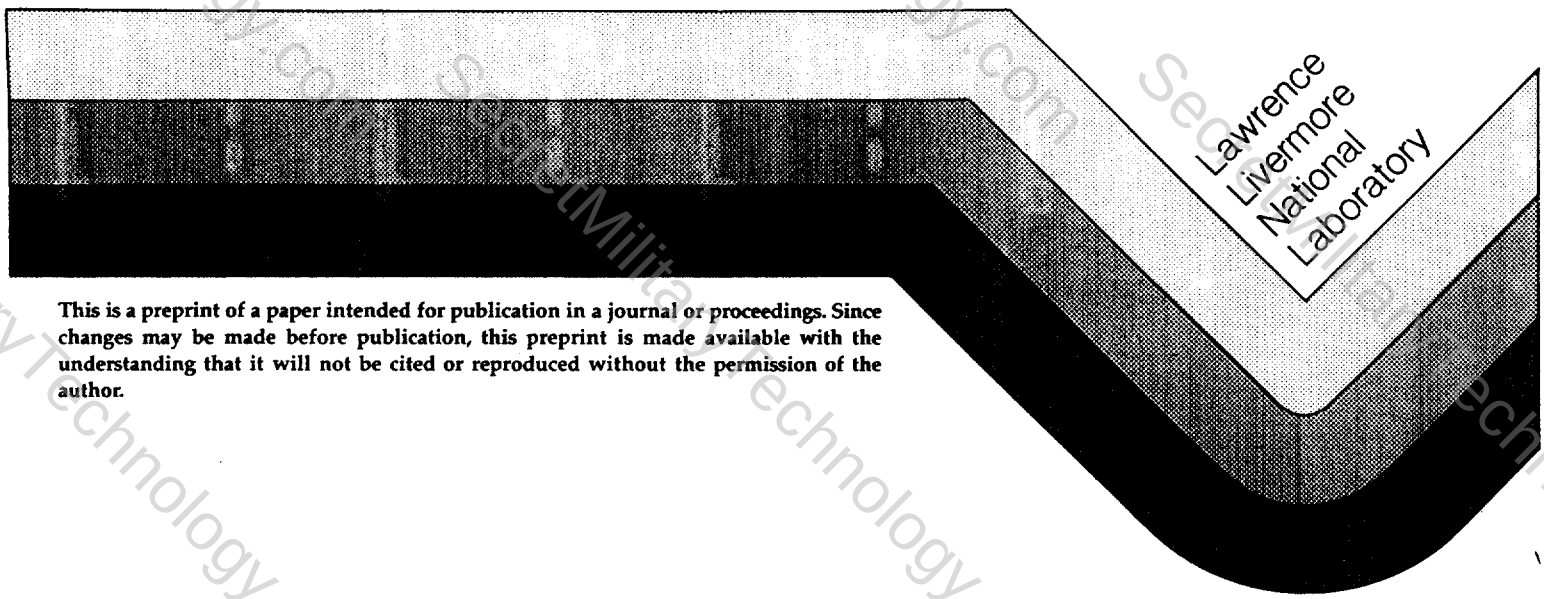

Acceleration of Compact Toruses and Fusion Applications*

C. W. Hartman, J. L. Eddleman, J. H. Hammer, B. G. Logan,
H. S. McLean, and A. W. Molvik

Lawrence Livermore National Laboratory
P.O. Box 808, L-637
Livermore, CA 94550

Abstract

The Compact Torus (Spheromak-type) is a near ideal plasma confinement configuration for acceleration. The fields are mostly generated by internal plasma currents, plasma confinement is toroidal, and the compact torus exhibits resiliency and stability in virtue of the "rugged" helicity invariant. Based on these considerations we are developing a coaxial rail-gun type Compact Torus Accelerator (CTA). In the CTA, the CT ring is formed between coaxial electrodes using a magnetized Marshall gun, it is quasistatically "precompressed" in a conical electrode section for inductive energy storage, it is accelerated in a straight-coaxial electrode section as in a conventional rail-gun, and it is focused to small size and high energy and power density in a final "focus" cone section.

The dynamics of slow precompression and acceleration have been demonstrated experimentally in the RACE device with results in good agreement with 2-D MHD code calculations. CT plasma rings with 100 μgms mass have been accelerated to 40 KJ kinetic energy at 20% efficiency with final velocity $\simeq 1 \times 10^8$ cm/s ($\simeq$ 5 KeV/H^+). Preliminary focus tests exhibit the predicted dynamics of radius compression, deceleration, and bouncing. Compression ratios of 2-3 have been achieved.

---

*Work performed under the auspices of the U.S. Department of Energy by the Lawrence Livermore National Laboratory under contract W-7405-ENG-48.

A scaled-up 10-100 MJ CTA is predicted to achieve a focus radius of several cm to deliver $\simeq$ 30 MJ ring kinetic energy in 5-10 nsec. This is sufficient energy, power, and power density to enable the CTA to act as a high efficiency, low cost ICF driver. Alternatively, the focused CT can form the basis for an magnetically insulated, inertial confinement fusion (MICF) system. Preliminary calculations of these fusion systems will be discussed.

I. Introduction

The acceleration of magnetically confined plasma with subsequent focusing offers the possibility of achieving very high power, power density and energy density with applications to soft x-ray generation, magnetically insulated ICF (MICF) and ICF. The mass of accelerated plasma, 10^{-5} to 10^{-2} gm, places this type accelerator intermediate between space-charge limited accelerators (electron ring, etc.) and conventional rail-gun accelerators. Typical kinetic energy per nucleon is 10-100 keV, in the range of thermonuclear fusion requirements, while the total energy of accelerated plasma in scaled up accelerators may be 10-100 MJ, in the range required for MICF and ICF. In this paper we discuss the Compact Torus Accelerator (CTA), the dynamics of accelerated CTs, experimental studies of the CTA, and proposed fusion applications.

II. Compact Torus Accelerator Concept and Compact Torus Dynamics

The coaxial rail-gun type CTA[1,2] discussed here is shown schematically in Fig. 1. The CT plasma ring acts as a moving short between the coaxial electrodes and is accelerated by the $\bar{j}_r \times \bar{B}_\theta$ force as in the usual rail-gun. Four phases of operation of the CTA are shown. First, the CT ring is formed using a magnetized plasma gun driven by a capacitor bank discharged across the outer two electrodes at the accelerator breach. The pre-established radial magnetic field shown in Fig. 1 is entrained by plasma and B_θ field emerging from the gun to form, after reconnection of the poloidal field, an isolated CT plasma ring shown in the formation phase of Fig. 1. Formation

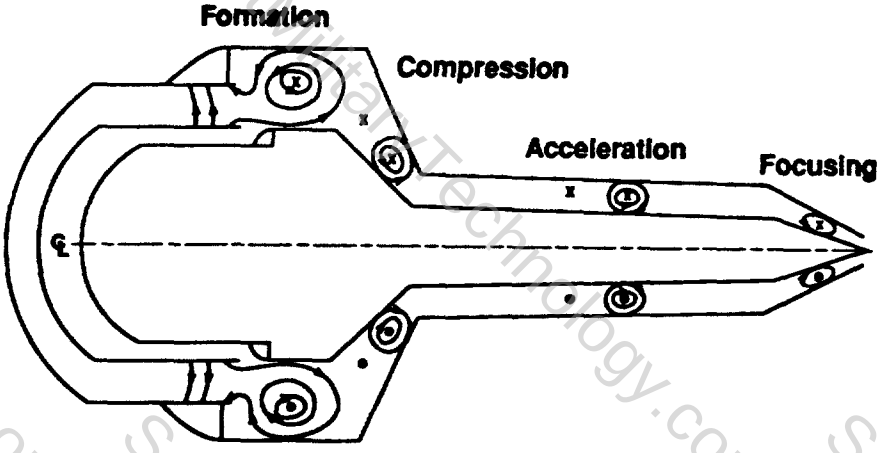

Fig. 1. Conceptual drawing of the Compact Torus Accelerator. The magnetized plasma gun utilizes the outer two coaxial electrodes at the accelerator breach.

can be fast ($\tau_{form} \simeq \tau_{Alfven}$) as done early in our experiments, or slow ($\tau_{form} \simeq \tau_{CT\ decay} >> \tau_{Alfven}$) by helicity injection as done presently in the experiments.

Following formation, an acceleration capacitor bank is discharged between the inner two electrodes at the breach and the CT ring can be accelerated directly between straight coaxial electrodes or quasistatically precompressed in a coaxial electrode section (compression region, Fig. 1). We have experimentally tested both direct acceleration and precompression.

Neglecting the plasma pressure ($\beta<<1$), the ring equation of motion is approximately,

$$M\ddot{\rho} = \dot{L}_{cone} I^2/2 - dU_m/d\rho - F_{drag} \qquad (1.)$$

where ρ is the ring position measured along the cone, $L'_{cone} I^2/2$ is the force of the accelerating B_θ field generated by accelerator current I with cone inductance per unit length L'_{cone} H/cm, U_m is the magnetic energy of the rings, $dU_m/d\rho$ is the component of the radial equilibrium force along the cone, $\alpha \sin\theta$ where $\theta = \theta(\rho)$ is the cone angle and F_{drag} is the drag force on the ring exerted by the electrodes. For quasistatic compression $M\ddot{\rho}$ and F_{drag} are $\simeq 0$ and the component of the radial equilibrium force along the cone $dU_m/d\rho$ is in near balance with the force of the accelerating B_θ field $L'_{cone} I^2/2$. Precompression can be slow ($\tau_{compression} \lesssim \tau_{CT\ decay}$) allowing the use of low voltage, low power capacitor banks to store energy inductively prior to acceleration. On the other hand, for efficient direct acceleration without precompression $dU_m/d\rho = 0$ and for efficient coupling, the circuit time constant $\sim\sqrt{(L_{ext} + L_{acc})C}$ must be about the same as the CT ring transit time L_{acc}/V_{ring} leading to low capacitance, high voltage driver banks because of the high velocity V_{ring} and low mass.

After precompression the ring enters the straight coax acceleration phase of Fig. 1. Here the equilibrium force is orthogonal to the electrode surfaces so that $dU_m/d\rho = 0$ and acceleration takes place limited by eddy current drag on the electrodes (F_{drag} in Eq. 1) and trailing plasma embedded on the accelerating field. The normalized force which can be applied to the CT ring for acceleration, $\kappa = (L'_{acc} I^2/2)/(U_m/L_{ring}) = (B^2_\theta/B^2_{CT})$ is limited to $\kappa<1$ by "blow by" of the accelerating field near the center electrode. The "blow-by" condition $\kappa = 1$ has been obtained by 2D MHD numerical computation and verified experimentally. A lower upper limit on $\kappa \lesssim 0.4$ has been predicted based on the destabilization of shear stabilized Rayleigh-Taylor ballooning modes of the CT ring[3] however, no clear evidence of this effect has been obtained experimentally.

A CT ring undergoing acceleration is predicted and observed to change shape as the poloidal field at the rear of the ring is compressed. In addition, during uniform acceleration, the plasma "slumps" to the rear of the ring assuming an exponential atmosphere distribution for the density $\rho = \pi(\Psi)$

$\exp(-\dot{v}_{ring} z/c_s^2)$ where $c_s^2 = T(\Psi)/m_i$.[2,4] Variation of the acceleration can provide strong heating of ions through "sloshing" of the plasma through interpenetrating ion orbits or shock waves at small mean free path.

After acceleration, the high velocity ring is injected into a conical focusing region at the muzzle of the accelerator as shown in Fig. 1. Here the terms $M\ddot{\rho}$ and $dU_m/d\rho$ in Eq. 1 are dominant and the ring is decelerated converting the kinetic energy into magnetic energy of the CT ring with the ring velocity going to zero at a radius compression ratio $R_a/R_f = 1 + U_k/U_m$ where R_a is the radius during acceleration, R_f is the stagnation radius, and U_k and U_m are the ring kinetic and magnetic energy at the entrance of the focus cone. Since $U_k/U_m \simeq 100$ is predicted, a large compression ratio can be achieved on the short timescale determined by the ring velocity to achieve very high power and energy density as shown in Fig. 2. Since the CT ring dwell time on the focus cone is very short, inertia prevents significant motion of the cone during focusing when the ring fields greatly exceed the usual material stress limits. For Fig. 2 the ring is assumed to be adiabatic so that focusing is self-similar which leads to further increases in energy and power density because of shortening of the ring length.

III. Experimental Studies of the CTA in the RACE Facility

We have carried out experimental demonstrations of the CT acceleration in the RACE (for Plasma Ring Accelerator Experiment) facility shown in Fig. 3. The magnetized ring-formation gun with inner and outer solenoids is driven by the 200 KJ fast bank shown and more recently a 260 KJ, 11 kV slow bank. The gun is ~70 cm long, 34 cm OD and ~20 cm ID. Located inside the gun center electrode is an accelerator electrode which passes through a shielded accelerator feed insulator and then extends 4 m at 20 cm diameter with a 2 m cone. The outer accelerator electrode is 50 cm diameter and as configured in Fig. 3 also has a 4 m straight section with a 2 m focus cone. The electrode assembly is located in a 5' diameter vacuum tank with a base pressure in the low 10^{-7} torr range. For plasma formation, 1-10 Atm- cm^3

of gas (usually H_2) is admitted by 8 fast acting pulse gas valves located midway along the gun electrode as shown in Fig. 3.

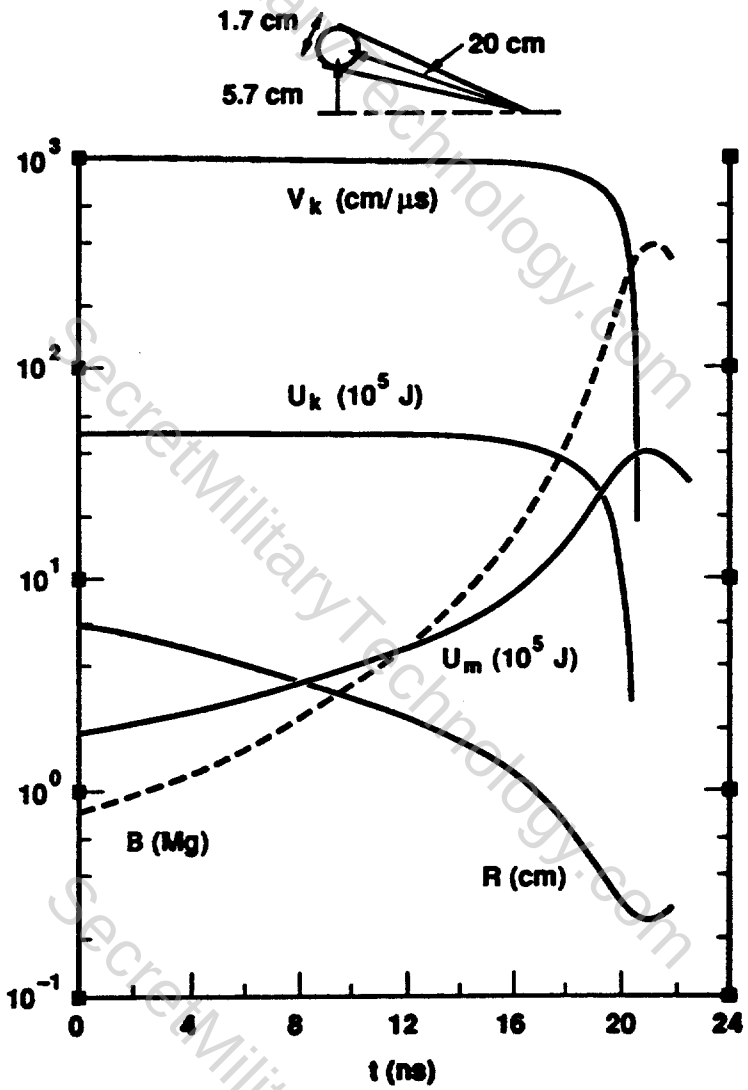

Fig. 2. High energy density focus example. A CT ring with $M = 10^{-4}$ gm, $V = 10^9$ cm/s, $U_k = 5$ MJ, $R = 5.7$ cm. The ring is assumed to undergo self-similar focusing.

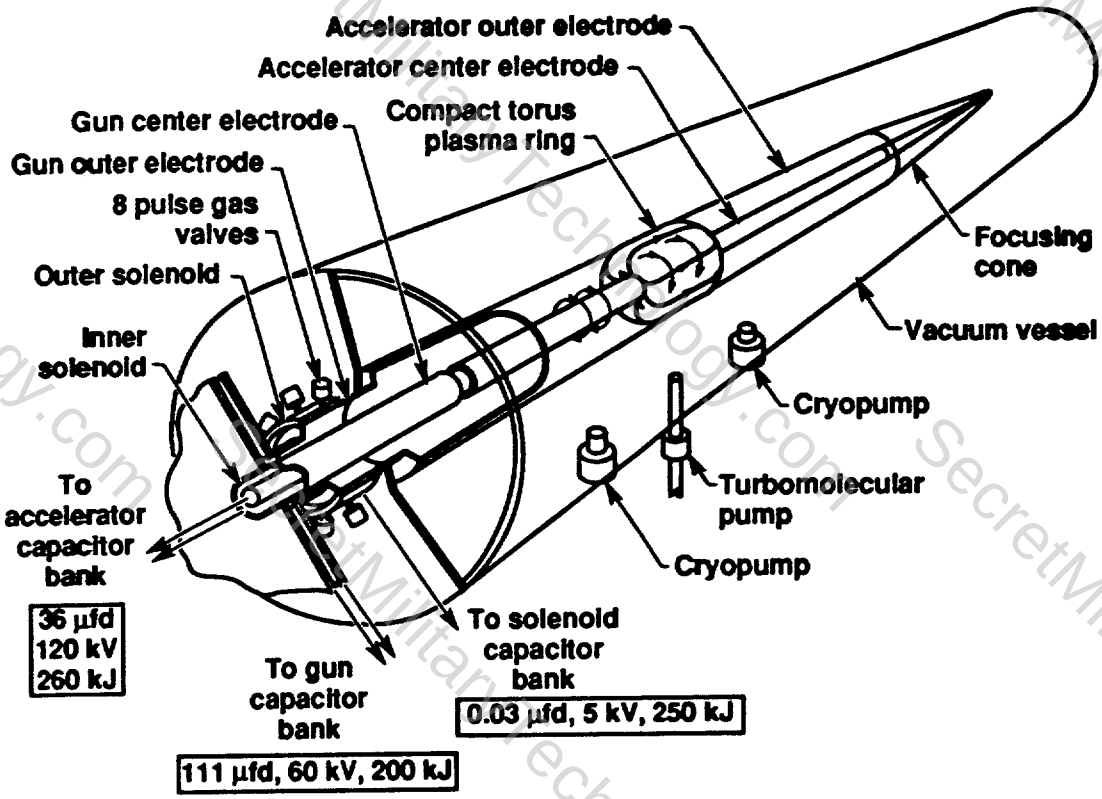

Fig. 3. Schematic of the RACE facility at LLNL. The accelerator electrodes, shown with a CT ring undergoing acceleration, are 4 m long with a 2 m focus cone section.

Initial experiments demonstrated the MHD model of CT ring formation with parameters L_{ring} = 50-100 cm, U_m = 2-10KJ, and V_{ring} = 20-50 cm/µs. The CT ring mass tended to be in the several x 10^{-4} gm range, dominated by O and C impurities. After successive electrode surface improvements by adding Ta liners and W spray coating and discharge cleaning, CT rings with M ≃ 10-20 µgm could be formed and accelerated.(5) The low mass, dominantly H^+ ion plasma rings could be formed only within

a limited range of parameter space with a critical dependence on forming the gun discharge just as the inlet gas crossed the interelectrode space.

Acceleration of low mass CT rings was achieved with trajectory results shown in Fig. 4. Here, the ring position along the accelerator is measured by B_z probes located at the outer electrode surface and the trajectory is compared with the current sheet position calculated from the accelerator inductance and the trajectory as calculated using the O-D RAC code. The RAC code solves Eq. 1 using external circuit parameters, it accounts for the CT ring field decay by calculating plasma energy flows to obtain the resistivity, and RAC utilizes an eddy current model for F_{drag}. The CT ring mass is assumed to be constant with M = 8 μgm used in Fig. 4, determined using a He Ne interferrometer at z = 120 cm. The agreement obtained in Fig. 4 shows that the the accelerator current flows at the ring position and that the trajectory, well described by RAC, is consistent with constant ring mass and a low drag force. For this shot the final ring velocity was $V_{ring} \sim 2 \times 10^8$ cm/s and the kinetic energy was U_k = 16 KJ as determined by the input energy to the accelerator and the RAC code.

The B_z and B_θ fields measured at the outer electrode by a probe at z = 124 cm are shown in Fig. 5. The B_θ field is seen to increase rapidly from t = 14 to 15 μs indicating a diffuse current sheath flowing at the back of the ring as expected from the current sheet trajectory. Further, the gradient of B_z has been steepened, as predicted, by the applied acceleration force. Fig. 6 shows the chord-averaged electron density for the same short shot indicating localization of the plasma density by the ring. For the conditions of this shot the plasma density both preceding and following the ring was below detectability $\bar{n}_e \lesssim 3 \times 10^{12}$ cm^{-3}. The results given by Figs. 4, 5, and 6 confirm the general 2-D, MHD model of CT ring acceleration.

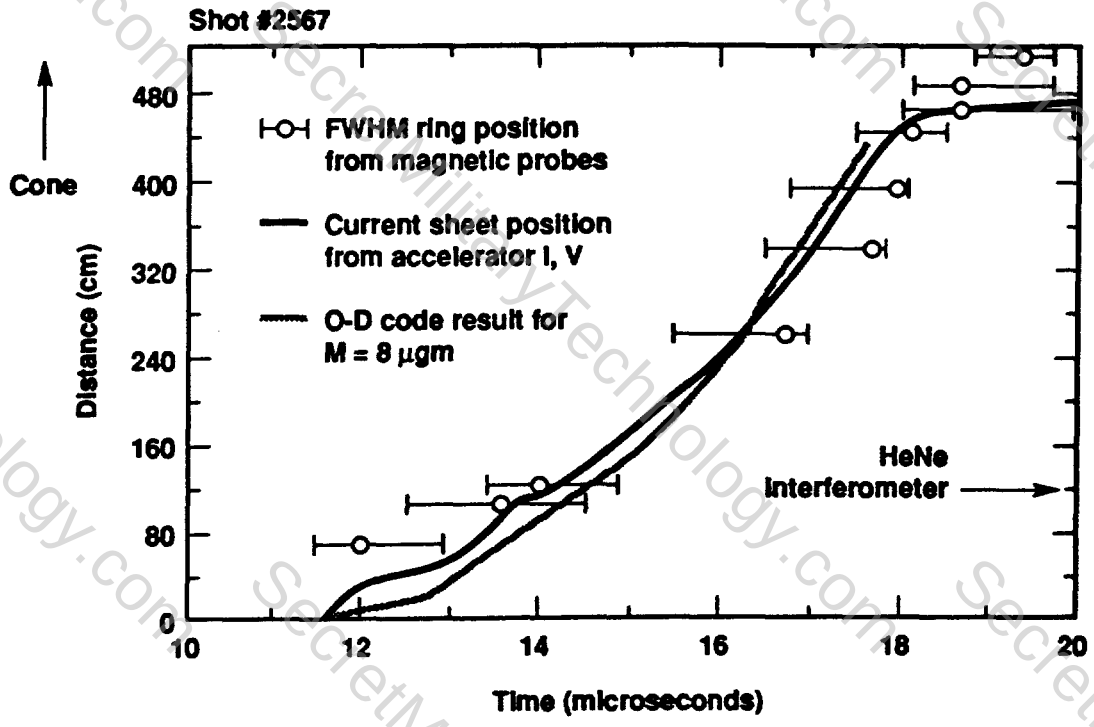

Fig. 4. CT ring trajectory. The barred data are B_Z at the outer accelerating electrode with O's at peak B_z and barr 1's at 1/2 B_{zpeak}. Note the shift of peak B_z to the back of the ring during strong acceleration (t = 16-18 μs). The current sheet position and trajectory calculated with the RAC O-D code are also shown.

Energy scaling studies have been conducted for direct acceleration with 5 m long acceleration electrodes. The studies were conducted over a number of shots in which the accelerator bank energy was gradually increased. Clean up of the electrode surfaces made it possible to achieve conditions for acceleration without strong trailing plasma interference both at higher bank energy and for early gas timing as well as late gas timing. For early gas timing, more efficient coupling in the gun was achieved and $U_m \simeq 10$ KJ could be achieved. The energy scaling results given in Fig. 7 correspond to a constant efficiency of 20% up to the maximum bank voltage of 100 kV. At 100 kV the accelerated ring parameters are $M \simeq 100$ μgm, $U_m \simeq 10$ KJ, $V_{ring} \simeq 10^8$ cm/s, and $U_k \simeq 40$ KJ.

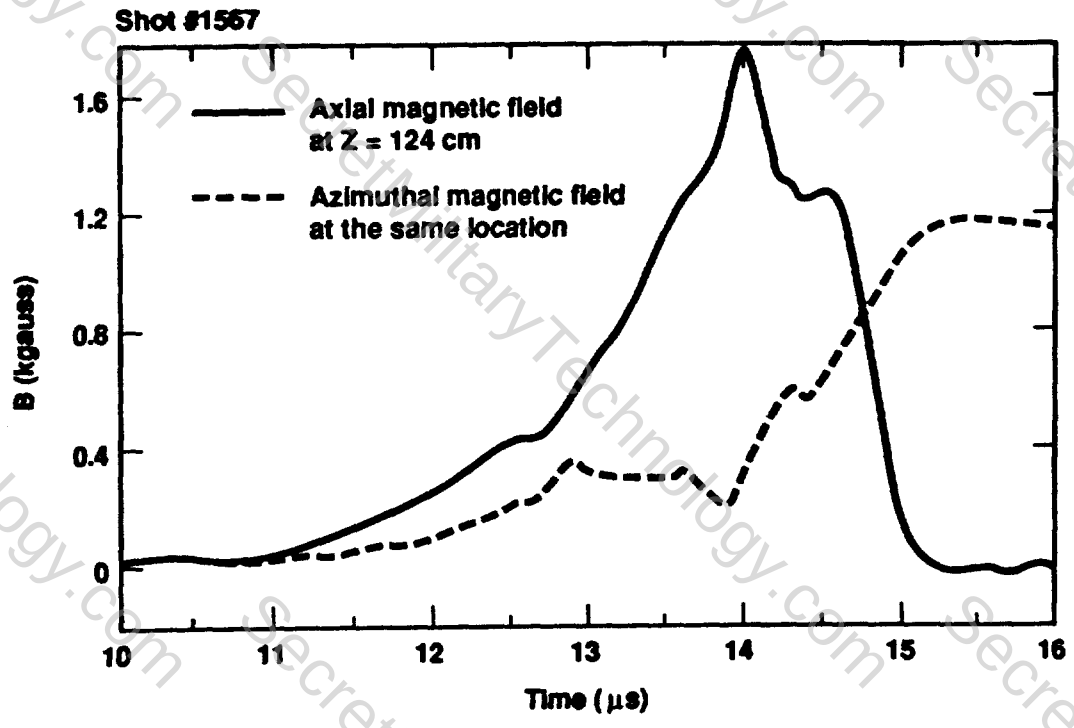

Fig. 5. Axial (B_z) and azimuthal (B_θ) fields measured at the surface of the outer electrode at z = 124 cm. Following energy scaling studies of direct acceleration, the accelerating electrodes were reconfigured as shown in Fig. 8 to test the precompression phase. The cone was dimensioned to provide 2:1 radial compression (R_{mean} 11.5 to 5.3 cm) and straight acceleration sections 1 m and 2 m long were used. The acceleration electrodes were made of copper and aluminum with W spray coating.

Because of the axial localization of the CT ring provided by the precompression cone, after initial fast formation tests, slow ring formation[6], $\tau_{form} \simeq 50$ μs, was employed. CT rings localized in the precompression cone have been formed with B_z up to 8 KG at the outer electrode entrance to the cone (z = 12 cm). The rings undergo stable, symmetric decay after the gun turns off with $\tau_{decay} \simeq 50$ μsec. Typical chord-averaged density is $\bar{n}_e \simeq$ few x 10^{15} cm^{-3} and the electron temperature inferred from τ_{decay} is a few tens of eV.

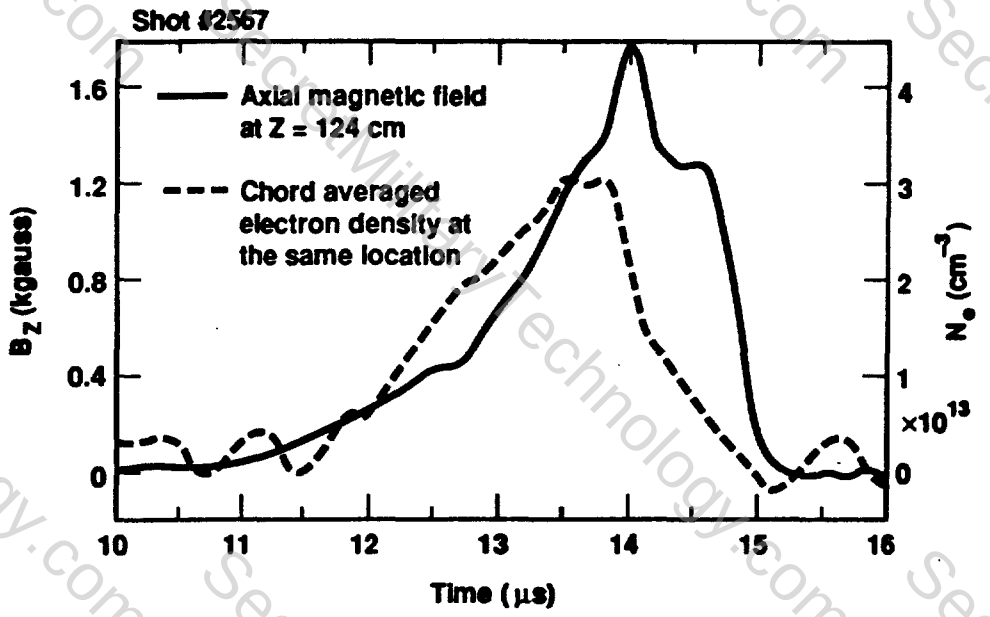

Fig. 6. Axial (B_θ) field shown in Fig. 5 and line-averaged electron density measured along a diameter at z = 124 cm.

The dynamics of precompression are in good agreement with ideal 2-D, MHD modeling using the Lagrangian TRAC code.[7] A comparison of data with the TRAC code predictions is shown in Fig. 9. The data were obtained with 1 μH external inductance in the accelerator bank circuit so that the current rises to peak current in ≃ 10 μs (t ≃ 49 μs, Fig. 9a). At t = 46 μs the B_z field at z = 12 cm decreases to ≃ 0 as the ring is compressed past z = 12 cm. At t ≃ 50 μs the compressed ring passes the small radius end of the cone (z = 43 cm) and enters the acceleration section where comparisons are made at z = 74 cm and z = 104 cm. Good quantitative agreement is obtained confirming the validity of the 2-D MHD model of precompression and acceleration. Compressed CT rings with M ≃ 100 μgm, $\bar{n}_e \simeq$ few x 10^{16} cm^{-3} B ≃ 20 KG, L_{ring} ≃ 30 cm have been formed and accelerated.

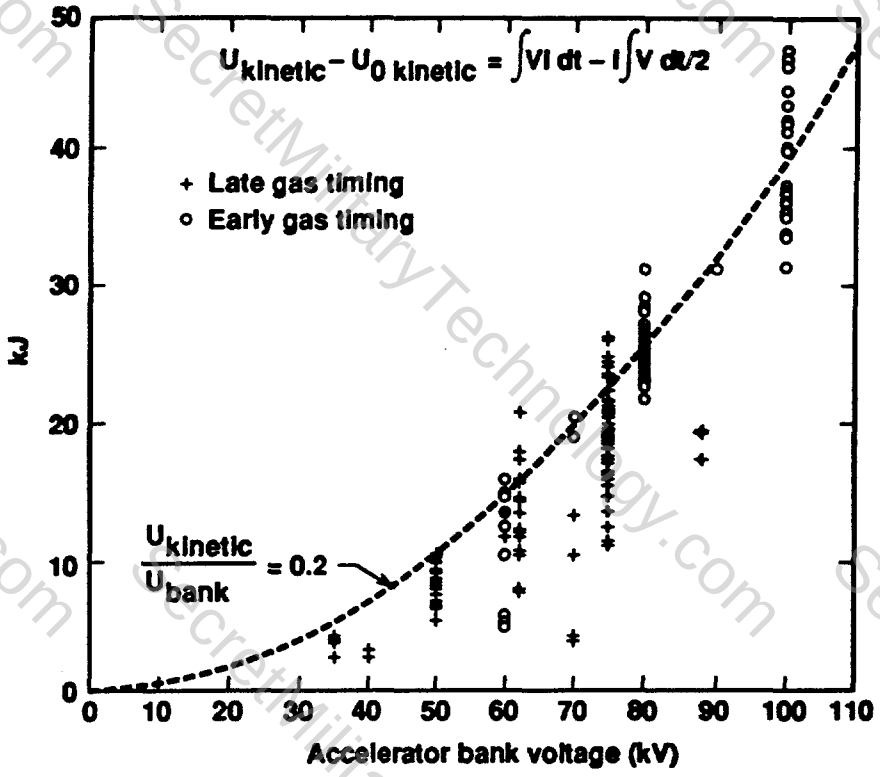

Fig. 7. Energy scaling results with 5 m straight electrodes in RACE. For early gas timing gas is admitted 300 μs before gun fire, for late timing 150 μs.

Our general conclusion from the experimental studies conducted thus far is that the compression and acceleration phases of the CTA can be described by the basic 2-D, MHD model discussed in Section III. Preliminary tests of CT ring focusing with the electrode configuration of Fig. 1 have been inconclusive. The general dynamics of ring compression, deceleration, and bouncing in the cone are observed but the scaling of field strength and ring length with compression ratio for an adiabatic MHD model with $L_{ring} << L_{cone}$ generally was not observed. For the experiment $L_{ring} \simeq 1/2\text{-}1/3\ xL_{cone}$ so that nonadiabatic effects can play a significant role. Further tests of focusing will be made with a new electrode set under construction with $L_{ring} \simeq (1/25)\ L_{cone}$.

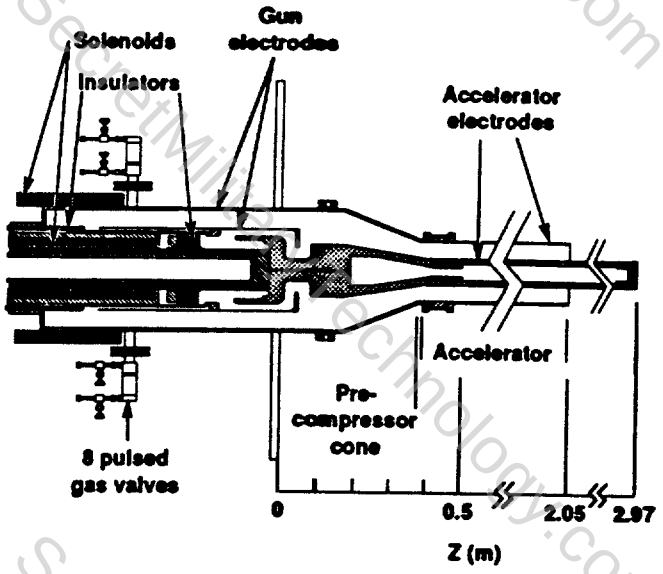

Fig. 8. RACE gun and accelerator electrodes with a precompression cone.

IV. CTA Scaling to High Energy and Fusion Applications

The MHD model of CT ring acceleration has been used to examine scaling of CTA's to high energy 10–100 MJ or so. The assumption is made that technical problems associated with electrode surfaces, etc. can be overcome by maintaining the surface energy and power density at allowable values and by keeping the field below $\simeq$ 200 kG (except for the focus cone where electrode destruction is expected each shot). A 100 MJ driver energy CTA has been considered which is predicted to produce 40 MJ kinetic energy CT rings which could be focused to of cm dimensions. Because of precompression, a low voltage driver bank can be used. The most significant cost item, the 500 kV, 100 MJ driver capacitor bank, has been estimated to cost 34M$ using off-the-shelf components. The over-all system cost is estimated to be $\simeq$ 3$/delivered joule.

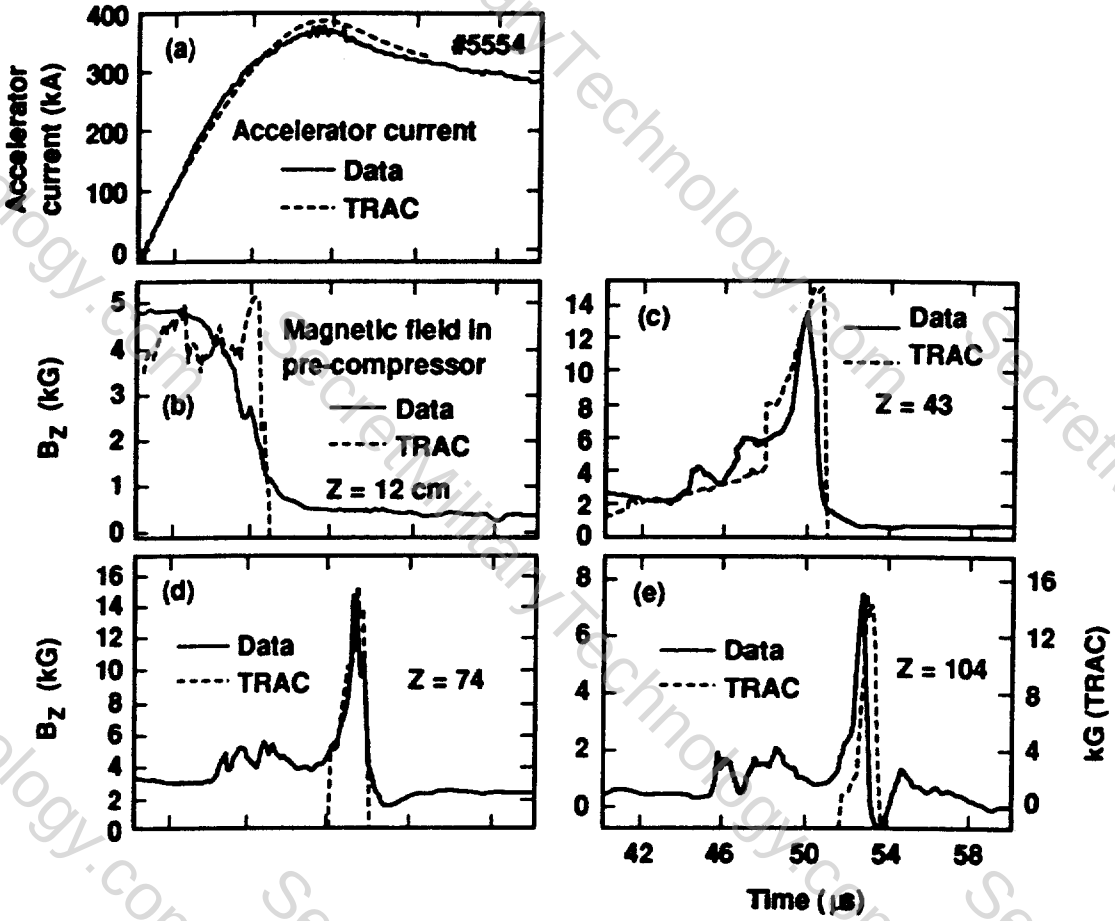

Fig. 9. A comparison of data with the precompression cone with TRAC a 2D, MHD Lagrangian code. Lack of coincidence at z = 104 cm is probably due to too high ring mass in the code.

IV. Fusion Applications

A high energy CTA which delivers 10^{15} watts/cm^2 of CT ring kinetic energy in 5-10 ns can act as a driver for an MICF[8] or ICF fusion system[9]. Interest in the CTA as a driver rests on high efficiency ~40%, basic simplicity,and on low cost. The accelerator would employ roughly a 100 cm to 20 cm radius precompression cone, a 30 m long acceleration section with $B_\theta \lesssim 200$ KG, and a 5 m long focus cone. The two fusion applications discussed here are shown in Fig. 10. Fig. 10a shows a "cannonball" MICF system. For this example a CTring with $U_k = 100$ MJ, $V_{CT} > 2 \times 10^8$ cm/s, $M_{CT} < 50$ mgm and $U_k/U_m \simeq 5\text{-}10$ is injected into a 1 cm radius cavity in the "cannonball" containment sphere. Shock waves generated by stagnation of the CT convert U_k into U_{plasma} at $T_i \simeq 10$ keV to initiate the DT thermonuclear burn. Since $U_k/U_m >> 1$, a transition to $\beta \simeq U_{plasma}/U_m > 1$ occurs and the plasma pressure is supported by the walls forming the MICF configuration.

In order to achieve gain $Q \gtrsim 20\text{-}30$, it is necessary to refuel the DT burn. Refueling in the example given here would be accomplished with DT fuel injection plugs driven by neutron absorption and heating of plug casings. Alternatively, high Q predicted by diffusive refueling if the containment chamber has an initial solid DT lining.[10] For a burn time $\tau_e \simeq 1$ μs a gain Q = 70 is predicted for the system considered to produce a total fusion yield of ~ 7 GJ. The containment "cannonball" is formed of Hg and has a thickness of several 14 MeV neutron mean-free-paths so that the yield is deposited in the cannonball which vaporizes and expands into a containment chamber to form the working gas for an MHD generator cycle.

The indirect-drive ICF application shown in Fig. 10b is estimated to require a 40 MJ kinetic energy CTring. Because of the high CTA efficiency, a gain $Q \simeq 50$ is adequate and a 2 GJ yield is estimated. Detailed design of the indirect drive capsule, including pulse shaping, is currently under study.

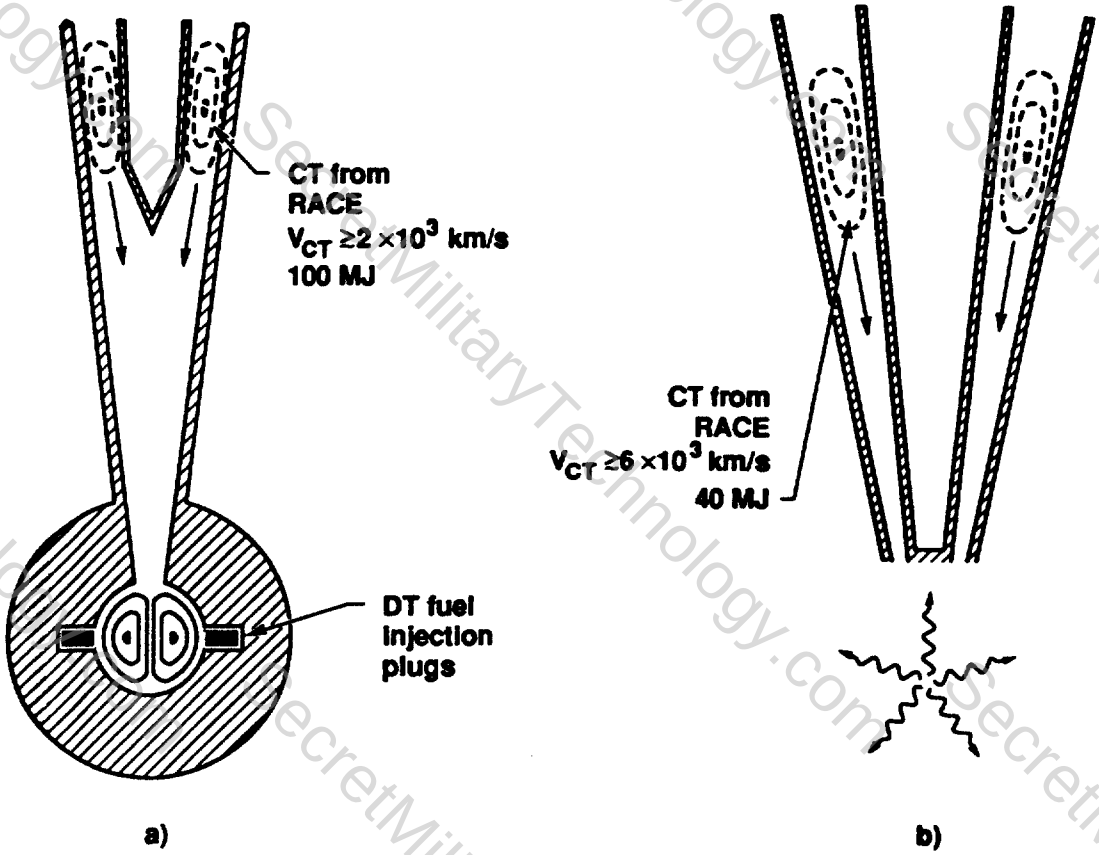

Fig. 10. Schematic drawings of possible MICF (Fig. 10a.) and ICF (Fig. 10b.) systems driven by the CTA. For MICF the fusion gain $Q \simeq 70$, $E_{fusion} \simeq 7$ GJ. The CT ring stagnation pressure is 100 Mb. For ICF $Q \simeq 50$, E_{fusion} 2 GJ. CTA driver costs are estimated to be 70M$ (MICF) and 35M$ (ICF).

References

1. C. W. Hartman and J. H. Hammer, Phys. Rev. Lett. 48, 929 (1982).

2. A. I. Morozov, "Equilibrium Configuration of a Uniformly Accelerating, Axisymmetric Plasma Configuration," J. of Tech. Phys. 37, No. 1, p. 79 (1967).

3. J. H. Hammer, J. L. Eddleman, and C. W. Hartman, Bull. Am. Phys. Soc. 30, 1449 (1985).

4. J. H. Hammer, private communication.

5. J. H. Hammer, C. W. Hartman, J. L. Eddleman, and H. S. McLean, Phys. Rev. Lett. 61, 2843 (1988).

6. T. R. Jarboe, et al, Phys. Fluids B 2, 1342 (1990).

7. J. L. Eddleman, et al, Bull. Am. Phys. Soc. 34, 2051 (1989).

8. A. Hasegawa, et al., "Magnetically Insulated and Inertially Confined Fusion MICF," Nuc. Fus. 28, No. 3, p. 369 (1988).

9. B. G. Logan, evaluation of MICF and ICF Systems.

10. T. Kammash, D. L. Galbraith, "A High Gain Fusion Reactor based on the Magnetically Insulated Inertial Confinement Fusion (MICF) Concept", J. Nuc. Fus. 29, No. 7, p. 1079 (1989).

Technical Information Department • **Lawrence Livermore National Laboratory**
University of California • Livermore, California 94551